Biogeosciences Discuss., https://doi.org/10.5194/bg-2017-328
Manuscript under review for journal Biogeosciences
Discussion started: 19 September 2017

Biogeosciences Discussions Open Access EGU

The devil's in the disequilibrium: sensitivity of ocean carbon storage to climate state and iron fertilization in a general circulation model

Sarah Eggleston[1,*] and Eric D. Galbraith[1,2,3]

[1]Institut de Ciència i Tecnologia Ambientals (ICTA), Universitat Autònoma de Barcelona, 08193 Barcelona, Spain
[2]Institució Catalana de Recerca i Estudis Avançats (ICREA), Pg. Lluís Companys 23, 08010 Barcelona, Spain
[3]Department of Earth and Planetary Science, McGill University, Montreal, Quebec H3A 2A7, Canada
[*]Now at: Laboratory for Air Pollution & Environmental Technology, EMPA, Überlandstrasse 129, 8600 Dübendorf, Switzerland

Correspondence to: S. Eggleston (sarah.eggleston@gmail.com)

Abstract. Ocean dissolved inorganic carbon (DIC) storage can be conceptualized as the sum of four components: saturation (DIC_{sat}), disequilibrium (DIC_{dis}), carbonate (DIC_{carb}) and soft tissue (DIC_{soft}). Among these, DIC_{dis} and DIC_{soft} have the potential for large changes that are relatively difficult to predict. Here we explore changes in DIC_{soft} and DIC_{dis} in a large suite of simulations with a complex coupled climate-biogeochemical model, driven by changes in orbital forcing, ice sheets and the radiative effect of CO_2. Both DIC_{dis} and DIC_{soft} vary over a range of 40 μmol/kg in response to the climate forcing, equivalent to changes in atmospheric CO_2 on the order of 50 ppm for each. We find that, despite the broad range of climate states represented, changes in global DIC_{soft} can be well-approximated by the product of deep ocean ideal age and the global export production flux, while global DIC_{dis} is dominantly controlled by the fraction of the ocean filled by Antarctic Bottom Water (AABW). Because the AABW fraction and ideal age are inversely correlated between the simulations, DIC_{dis} and DIC_{soft} are also inversely correlated. This inverse correlation could be decoupled if changes in deep ocean mixing were to alter ideal age independently of AABW fraction, or if independent ecosystem changes were to alter export and remineralization, thereby modifying DIC_{soft}. As an example of the latter, iron fertilization causes DIC_{soft} to increase, and causes DIC_{dis} to also increase by a similar or greater amount, to a degree that depends on climate state. We propose a simple framework to consider the global contribution of $DIC_{soft} + DIC_{dis}$ to ocean carbon storage as a function of the surface preformed nitrate and DIC_{dis} of dense water formation regions, the global volume fractions ventilated by these regions, and the global nitrate inventory. More extensive sea ice increases DIC_{dis}, and when sea ice becomes very extensive it also causes significant O_2 disequilibrium, which may have contributed to reconstructions of low O_2 in the Southern Ocean during the glacial. Global DIC_{dis} reaches a minimum near modern CO_2 because the AABW fraction reaches a minimum, which may have contributed to preventing further CO_2 rise during interglacial periods.

Biogeosciences Discuss., https://doi.org/10.5194/bg-2017-328
Manuscript under review for journal Biogeosciences
Discussion started: 19 September 2017

1 Introduction

The controls on ocean carbon storage are not yet fully understood. Although potentially very important, given the large inventory of dissolved inorganic carbon (DIC) the ocean contains (38,000 Pg C vs. 700 Pg C in the pre-industrial atmosphere), the nuances of carbon chemistry, the dependence of air-sea exchange on wind stress and sea ice cover, the intricacies of ocean circulation and the activity of the marine ecosystem all contribute to making it a very complex problem. The scale of the challenge is such that, despite decades of work, the scientific community has not yet been able to satisfactorily quantify the role of the ocean in the natural variations of CO_2 between 180 and 280 ppm that occurred over ice age cycles. This failure reflects persistent uncertainty that also impacts our ability to accurately forecast future ocean carbon uptake.

In order to help with process understanding, DIC can be theoretically divided among four components that, together, determine the air-sea partitioning of the "active" carbon inventory: DIC_{sat}, DIC_{dis}, DIC_{soft} and DIC_{carb} (Ito and Follows, 2013; Bernardello et al., 2014). The first two components are defined in the surface ocean and are carried passively by ocean circulation in the interior, while the latter two are equal to zero in the surface layer and accumulate in the interior due to biogeochemical activity.

Saturation DIC (DIC_{sat}) is simply determined by the atmospheric CO_2 concentration and its solubility in seawater, which is a function of ocean temperature, salinity, and alkalinity. For example, cooling the ocean will increase CO_2 solubility, thereby leading to an increase in DIC_{sat}. Given known changes in temperature, salinity, alkalinity, and atmospheric CO_2, the effective storage of DIC_{sat} can be calculated precisely.

The soft tissue pump (see e.g. Toggweiler et al., 2003) has been defined in various ways, but universally involves the uptake of DIC in the surface ocean by marine primary producers. The organic carbon that is formed then sinks or is subducted (as dissolved or suspended organic matter) and is transformed into remineralized DIC within the water column (a small fraction is buried at depth). Here we define DIC_{soft} as that accumulated by the net respiration of organic matter below the top layer of the ocean (in our model, the uppermost 10 m). Thus, DIC_{soft} depends both on the export flux of organic matter, affected by surface ocean conditions including iron supply (Martin, 1990), and on the flushing rate of the deep ocean, which clears out accumulated DIC_{soft} (Toggweiler et al., 2003). The Southern Ocean (SO) is thought to be an important region for such changes on glacial/interglacial timescales, as the ecosystem there is currently iron-limited, and it also plays a major role in deep ocean ventilation (Martin, 1990; Toggweiler et al., 2003; Jaccard et al., 2016); furthermore, the degree of stratification may have changed significantly on these timescales (François et al., 1997; Sigman et al., 2010). Assuming a constant global oceanic phosphate inventory and constant C:P ratio, DIC_{soft} would be stoichiometrically related to the preformed PO_4 ($PO_{4_{pre}}$) inventory of the ocean, where $PO_{4_{pre}}$ is the concentration of PO_4 in newly-subducted waters, and a passive tracer in the interior. The potential to use $PO_{4_{pre}}$ as a metric of DIC_{soft} prompted significant efforts to understand how it could change over time (Ito and Follows, 2005; Marinov et al., 2008a; Goodwin et al., 2008), though it has been pointed out that the large variation in C:P of organic matter weakens the relationship between DIC_{soft} and $PO_{4_{pre}}$ (Galbraith and Martiny, 2015). Dissolved O_2 can potentially serve as a better metric of DIC_{soft}, given the relatively small variations in the O_2:C of respiration compared to the relatively high variability in C:P (Martiny et al., 2013). But Apparent Oxygen Utilization (AOU), typically taken as a measure

Biogeosciences Discuss., https://doi.org/10.5194/bg-2017-328
Manuscript under review for journal Biogeosciences
Discussion started: 19 September 2017

of accumulated respiration, can be misleading if the preformed O_2 concentration differed significantly from saturation (Ito et al., 2004; Duteil et al., 2013). Thus, despite being conceptually simple, DIC_{soft} can be difficult to quantify observationally.

Similar to DIC_{soft}, DIC_{carb} is defined here as the DIC generated by the dissolution of calcium carbonate shells below the ocean surface layer. Note that this does not include the impact that shell production has at the surface; calcification causes alkalinity to decrease in the surface ocean, raising surface pCO_2 and shifting carbon to the atmosphere. Rather, within the framework used here, this effect on alkalinity distribution falls under DIC_{sat}, since it alters the solubility of DIC. Changes in DIC_{carb} on the timescales of interest are generally thought to be small compared to those of DIC_{sat} and DIC_{soft}.

Typically, only these three components are considered as the conceptual drivers behind changes in the air-sea partitioning of pCO_2 (e.g., IPCC, 2007; Kohfeld and Ridgwell, 2009; Marinov et al., 2008a; Goodwin et al., 2008). However, a fourth component, disequilibrium carbon (DIC_{dis}), is also potentially significant as discussed by Ito and Follows (2013). Defined as the difference between preformed DIC and DIC_{sat}, DIC_{dis} can be relatively large (Takahashi et al., 2009) because of the slow timescale of atmosphere-surface ocean equilibrium of carbon compared to other gases, caused by the buffering capacity of seawater (e.g., Zeebe and Wolf-Gladrow, 2001; Broecker and Peng, 1974).

Like DIC_{sat}, DIC_{dis} is a conservative tracer determined in the surface ocean, with no sources or sinks in the ocean interior. Since the majority of the ocean is filled by water originating from small regions of the Southern Ocean and the North Atlantic, the net whole-ocean disequilibrium carbon is approximately determined by the DIC_{dis} in these areas weighted by the fraction of the ocean volume filled from each of these sites. Unlike the other three components, DIC_{dis} could contribute either additional oceanic carbon storage ($DIC_{dis} > 0$) or reduced oceanic carbon storage ($DIC_{dis} < 0$). Studies using preformed nutrients as a metric for biological carbon storage have often ignored the potential importance of DIC_{dis} by assuming fast air-sea gas exchange (e.g., Marinov et al., 2008a; Ito and Follows, 2005). In the pre-industrial ocean this is of little importance, given that global DIC_{dis} is small because the opposing effects of North Atlantic and Antarctic water masses largely cancel each other. However, Ito and Follows (2013) showed that DIC_{dis} can have a large impact by amplifying changes in DIC_{soft} under constant pre-industrial ocean circulation, and the possibility that DIC_{dis} varied in response to changes in ocean circulation states has not been thoroughly explored.

Here, we use a fully-coupled general circulation model (GCM) to investigate the potential importance of DIC_{dis} in altering air-sea CO_2 partitioning on long timescales. We make use of a large number of equilibrium simulations, conducted over a wide range of CO_2, orbital and ice sheet boundary conditions, as a "library" of contrasting ocean circulations in order to test the response of disequilibrium carbon storage to physically plausible changes in ocean circulation. We supplement these with a smaller number of iron fertilization experiments to examine the additional impact of ecosystem changes. In order to simplify the interpretation, we chose to prescribe a constant CO_2 for the air-sea exchange in all simulations. Thus, the changes in DIC_{sat} reflect only changes in temperature, salinity, alkalinity and ocean circulation, and not changes in pCO_2. Nor do they explicitly consider changes in the total carbon or alkalinity inventories, although these may have changed significantly due to changes in outgassing and/or burial (Roth et al., 2014; Tschumi et al., 2011). As such, the experiments here should be seen as idealized climate-driven changes, and should be further tested with more comprehensive models including interactive CO_2.

Biogeosciences Discuss., https://doi.org/10.5194/bg-2017-328
Manuscript under review for journal Biogeosciences
Discussion started: 19 September 2017

2 Methods

2.1 Model description

The GCM used in this study is CM2Mc, the Geophysical Fluid Dynamics Laboratory's Climate Model version 2 but at lower resolution (3°), described in more detail by Galbraith et al. (2011). This includes the Modular Ocean Model version 5, a sea ice module, static land and ice sheets, and a module of Biogeochemistry with Light, Iron, Nutrients and Gases (BLINGv1.5) (Galbraith et al., 2010). Unlike BLINGv0, BLINGv1.5 allows for variable stoichiometry and calculates the mass balance of phytoplankton in order to prevent unrealistic bloom magnitudes at high latitudes, reducing the magnitude of disequilibrium O_2, which was very high in BLINGv0 (Duteil et al., 2013; Tagliabue et al., 2016).

2.2 Experimental design

The basic setup of all model runs is identical to Galbraith and de Lavergne (submitted). A control run was conducted with atmospheric CO_2 set to 270 ppm and the Earth's obliquity and precession set to modern values (23.4° and 102.9°, respectively). Experimental simulations were run at values of obliquity (22°, 24.5°) and precession (90°, 270°) representing the astronomical extremes encountered over the last 5 My (Laskar et al., 2004). Solar radiation was varied at CO_2 levels equivalent to 180, 220, 270, 405, 607, and 911 ppm. The biologeochemical component of the model calculates air-sea carbon fluxes using a fixed atmospheric CO_2 of 270 ppm throughout all model runs, irrespective of the CO_2 used for radiative forcing.

Eight additional runs were conducted using Last Glacial Maximum (LGM) ice sheets with CO_2 of 180 and 220 ppm and the same orbital parameters. Iron fertilization simulations use the glacial atmospheric dust field of Nickelsen and Oschlies (2015) instead of the standard pre-industrial dust field. Four iron fertilization experiments were run at an atmospheric CO_2 of 180 ppm with LGM ice sheets, as well as one model run similar to the control run. Finally, two simulations were run that were identical to the pre-industrial setup, but the rate of remineralization of sinking organic matter is set to 75% of the default rate, approximately equivalent to the expected change due to a 5°C ocean cooling (Matsumoto et al., 2007); one of these runs also includes iron fertilization. All simulations are summarized in Table 1.

The simulations were run for 2100 – 6000 model years beginning with a pre-industrial spinup. While the model years presented here largely reflect runs after having reached steady state, it is important to note that the pre-industrial run (41 in Table 1) still has a drift of 1 μmol/kg over the 100 y shown here and thus may not yet be at steady state.

2.3 DIC decomposition

Following Ito and Follows (2013) and Bernardello et al. (2014), we separate the total DIC into preformed and remineralized DIC (DIC_{pre} and DIC_{rem}).

$$DIC = DIC_{pre} + DIC_{rem} \quad (1)$$

DIC_{pre} is set equal to DIC at the surface and is propagated into the ocean interior as a conservative tracer. It in turn is the sum of two components: the first is the DIC at equilibrium with the atmosphere (DIC_{sat}), and the second is the disequilibrium

Biogeosciences Discuss., https://doi.org/10.5194/bg-2017-328
Manuscript under review for journal Biogeosciences
Discussion started: 19 September 2017

term, defined as the degree of under- or oversaturation (DIC_{dis}). Note that in all simulations, DIC_{sat} is calculated using a CO_2 concentration of 270 ppm, as this was prescribed identically for the biogeochemical component in all simulations, as discussed above. The use of a constant CO_2 concentration for biogeochemistry is not consistent with the CO_2 used for radiative forcing, which changes between simulations, but it provides a relatively simple framework for comparison of this large suite of simulations.

$$DIC_{pre} = DIC_{sat} + DIC_{dis} \tag{2}$$

Within the mixed layer, plankton take up DIC to produce organic matter or calcium carbonate shells, both of which sink or are subducted and are remineralized in the water column to inorganic carbon (DIC_{soft} and DIC_{carb}, respectively).

$$DIC_{rem} = DIC_{soft} + DIC_{carb} \tag{3}$$

DIC_{sat}, DIC_{soft}, and DIC_{carb} can be calculated explicitly from the model tracers (for more details, see the appendix), and DIC_{dis} is then calculated as a residual.

$$DIC_{dis} = DIC - DIC_{sat} - DIC_{soft} - DIC_{carb} \tag{4}$$

3 Results

3.1 Climate experiments

Total DIC generally decreases from cold to warm simulations, under the constant CO_2 of 270 ppm used for air-sea exchange. Changes in DIC_{sat} drive the largest portion of this trend, decreasing approximately linearly with $\ln(CO_2)$ due to the temperature-dependence of CO_2 solubility, resulting in a difference of 50 μmol/kg over this range (see fig. 1). DIC_{carb} is small in magnitude with a standard deviation of only 4 μmol/kg over the entire range of CO_2 values, and we do not discuss it further.

In contrast to DIC_{sat}, DIC_{dis} and DIC_{soft} vary nonlinearly with global temperatures, with a clear and shared turning point at a radiative forcing near a CO_2 concentration of about 400 ppm. Both DIC_{dis} and DIC_{soft} are strongly correlated with ocean ventilation, quantified here by the global average of the ideal age tracer (r^2 = 0.69 and 0.89, respectively), and thus with each other (r^2 = 0.74). However, in contrast to the findings of Ito and Follows (2013), who found a positive correlation of DIC_{soft} and DIC_{dis} under nutrient depletion experiments with constant climate, DIC_{soft} and DIC_{dis} are negatively correlated under the range of climate states under constant iron supply explored here.

3.2 Iron fertilization experiments

The impact of increasing the dust flux to the ocean on DIC_{soft} depends strongly on the ocean circulation state (see fig. 2). In the pre-industrial climate state (middle panel), half of the total oceanic C inventory change (14.6 μmol/kg) is due to increased soft tissue pump storage (ΔDIC_{soft} = 7.3 μmol/kg). This is qualitatively the same in the case that the remineralization rate of organic carbon is reduced by 25% (left panel). However, in the high-ventilation runs under glacial-like conditions (right panel),

Biogeosciences Discuss., https://doi.org/10.5194/bg-2017-328
Manuscript under review for journal Biogeosciences
Discussion started: 19 September 2017

the change in total DIC is somewhat reduced (11.1 μmol/kg) and ΔDIC_{soft} is small (SO average 4.3 μmol/kg; global average 2.9 μmol/kg). DIC_{dis} is also dependent on the ocean circulation, but in the opposite direction: the change is more significant (9.4 μmol/kg global average) in the glacial-like simulations compared to the pre-industrial simulation (6.4 μmol/kg). Each of these values rises when considering only the SO (13.4 and 9.0 μmol/kg, respectively). In both the pre-industrial and glacial-like simulations, changes in DIC_{dis} constitute an important part of the total change. DIC_{carb} is reduced to a small extent by iron fertilization, due to the reduced nutrient content of AAIW/SAMW and consequent decrease in low latitude carbonate production, which raises low latitude surface ocean alkalinity, causing an increase in DIC_{sat}.

4 Discussion

Simulated changes in DIC_{dis} are of the same magnitude as the DIC_{soft} changes, to which much greater attention has been paid. For a global average buffer factor between 8 and 14 (Zeebe and Wolf-Gladrow, 2001), a rough, back-of-the-envelope calculation shows that a 1 μmol/kg change in DIC corresponds to a 0.9 – 1.6 ppm change in atmospheric pCO_2 based on a DIC concentration of 2300 μmol/kg and CO_2 of 270 ppm. Thus, the increase in the global average DIC_{dis} in these simulations of 16 μmol/kg (pre-industrial control) to 62 μmol/kg (LGM-like conditions with Fe fertilization) could have contributed the equivalent of a 40 – 70 ppm change in the atmospheric CO_2 stored in the ocean during the glacial compared to today. It is important to recognize that the drawdown of CO_2 by disequilibrium storage would have resulted in a decrease of DIC_{sat}, given the dependence of the saturation concentration on pCO_2, so this estimate should not be interpreted as a straightforward atmospheric CO_2 change. Nonetheless, while this is only a first-order approximation and the model biases are potentially large, it seems very likely that the desquilibrium carbon storage was a significant portion of the net 90 ppm difference.

Below, we discuss the changes in DIC_{soft} and DIC_{dis} that result from the CO_2, orbital and ice-sheet driven climate changes. We then discuss related changes in disequilibrium O_2, implications for preformed nutrient theory, and propose a new mechanism that may have helped to prevent the Earth from warming its way out of the ice age cycle.

4.1 Climate-driven changes in DIC_{soft}

The biogeochemical model used here is relatively complex, with limitation by three nutrients (N, P and Fe), denitrification and N_2 fixation, in addition to the temperature- and light-dependence typical of biogeochemical models. The climate model is also complex, including a full atmospheric model, a highly-resolved dynamic ocean mixed layer, and many nonlinear subgridscale parameterizations, and uses short (< 3 h) timesteps. The simulations we show span a wide range of behaviours, including major changes in ocean ventilation pathways and patterns of organic matter export.

Thus, it is perhaps surprising that the net global result of the biological pump, as quantified by DIC_{soft}, has highly predictable behavior. As shown in fig. 3, the global DIC_{soft} varies closely with the product of the global sinking flux of organic matter at 100 m and the ideal age of the global ocean. Qualitatively this is not a surprise, given that greater export pumps more organic matter to depth, and a large age provides more time for respired carbon to accumulate within the ocean. But the quantitative strength of the relationship is striking.

Biogeosciences Discuss., https://doi.org/10.5194/bg-2017-328
Manuscript under review for journal Biogeosciences
Discussion started: 19 September 2017

It is difficult to assess the likelihood that the real ocean follows this relationship to a similar degree. One reason it might differ is if remineralization rates vary spatially, or with climate state. In the model here, as in most biogeochemical models, organic matter is respired according to a globally-uniform power law relationship vs. depth (Martin et al., 1987). Kwon et al. (2009) showed that ocean carbon storage is sensitive to changes in these remineralization rates, and this would provide an additional degree of freedom. It is not currently known how much remineralization rates can vary naturally; they may vary as a function of temperature (Matsumoto et al., 2007) or ecosystem structure. As a result, the relationship between DIC_{soft} and ideal ocean age multiplied by global export may be stronger in the model than in the real ocean.

Nonetheless, the results suggest that, as a useful first-order approximation, the global change in DIC_{soft} between two states can be given by a simple linear regression:

$$\Delta DIC_{soft}[\mu mol\ kg^{-1}] = 0.036 \cdot \Delta(export[Pg\ C\ y^{-1}] \cdot age[y]) \quad (5)$$

or in CO_2 terms and assuming a buffer factor of 10:

$$\Delta CO_{2,soft}[ppm] \approx m \cdot \Delta(export[Pg\ C\ y^{-1}] \cdot age[y]) \quad (6)$$

where $m = 0.065, 0.042, 0.029$ for modern, pre-industrial and glacial conditions respectively. This simple meta-model may provide a useful substitute for full ocean-ecosystem calculations, and could be further tested against other ocean-ecosystem coupled models. Note that, as for the disequilibrium estimate above, the soft tissue pump CO_2 drawdown would be partially compensated by a decrease in saturation carbon storage, so this should not be interpreted as a net atmospheric effect. In addition, we have not accounted for consequent changes in the surface ocean carbonate chemistry (including changes in the buffer factor). It would be useful to check this relationship with models including interactive CO_2.

It is important to point out that the simulated change in DIC_{soft} between interglacial and glacial states is in conflict with reconstructions. Proxy records appear to show that LGM dissolved oxygen concentrations were lower throughout the global ocean, with the exception of the North Pacific, implying greater DIC_{soft} concentrations during the glacial then during the Holocene (Galbraith and Martiny, 2015). In contrast, the model suggests that greater ocean ventilation rates in the glacial state would have led to reduced global DIC_{soft}. As discussed by Galbraith and de Lavergne (submitted), radiocarbon observations imply that the model ideal age is approximately 200 y too young under glacial conditions, compared to the LGM, suggesting a circulation bias that may reflect incorrect diapycnal mixing or non-steady-state conditions. Whatever the cause, if we take this 200 y bias into account, the regression implies an additional 33 $\mu mol\ kg^{-1}$ DIC_{soft} were stored in the glacial ocean. This would bring the simulated glacial DIC_{soft} close to, but still less than, the simulated pre-industrial value. We propose that the apparent remaining shortfall in simulated glacial DIC_{soft} could reflect one or more of the following non-exclusive possibilities: 1. the model does not capture changes in remineralization rates caused by ecosystem changes; 2. the model underestimates the glacial increase in the nitrate inventory, perhaps due to changes in the iron cycle; 3. the ocean was not in steady state during the LGM, and therefore not directly comparable to the "glacial" simulation; 4. the inference of DIC_{soft} from proxy oxygen records is incorrect due to significant changes in preformed oxygen disequilibrium (see below). If either of the first two possibilities is important, it would imply an inaccuracy in the meta-model derived here.

Biogeosciences Discuss., https://doi.org/10.5194/bg-2017-328
Manuscript under review for journal Biogeosciences
Discussion started: 19 September 2017

4.2 Climate-driven changes in DIC_{dis}: volume fractions

The ocean basins below 1 km depth are largely filled by surface waters subducted to depth in regions of deepwater formation (Gebbie and Huybers, 2011). In our simulations, water originating in the surface North Atlantic, termed NADW, and the Southern Ocean, termed AABW, make up 80-96% of this total deep ocean volume. Thus, to first order, the deep average DIC_{dis} concentration can be approximated by a simple mass balance:

$$DIC_{dis_{deep}} \approx f_{AABW} \cdot DIC_{dis_{AABW}} + f_{NADW} \cdot DIC_{dis_{NADW}} \quad (7)$$

Here, f_{AABW} and f_{NADW} represent the fraction of deepwater originating in the SO and North Atlantic and $DIC_{dis_{AABW,NADW}}$ the DIC_{dis} concentration at the sites of deepwater formation (see fig. 4). North Atlantic deep waters form with negative DIC_{dis}, reflecting surface undersaturation, while the Southern Ocean is supersaturated ($DIC_{dis} > 0$), and these opposing tendencies between NADW and AABW cause a partial cancellation of DIC_{dis} when globally averaged. Although the exact values of DIC_{dis} in the two polar oceans vary over time in response to climate (the reasons for which are discussed in more detail below), these changes are small relative to the consistent large contrast between AABW and NADW, so that deep DIC_{dis} is strongly controlled by the global balance of AABW vs. NADW in each simulation (see fig. 5). Global DIC_{dis} becomes much larger when f_{AABW} is larger, similar to the dynamic evoked by Skinner (2009).

In this model, both the cold and the hot climate states show increased AABW production, with a minimum at intermediate values. The AABW/NADW fractions are determined by the relative density of surface waters in the two polar ocean basins, as discussed in more detail by Galbraith and de Lavergne (submitted). The minimum in AABW is thus responsible for the minimum in global ocean DIC_{dis} (fig. 1). In addition, expanded terrestrial ice sheets shift the ratio of AABW to NADW to higher values, due to their impact on NADW temperature and downstream expansion of Southern Ocean sea ice (Galbraith and de Lavergne), further increasing DIC_{dis} in glacial-like conditions.

4.3 Climate-driven changes in DIC_{dis}: end members

Due to the general dominance of AABW in the deep ocean, the concentration of DIC_{dis} in the regions of AABW formation, $DIC_{dis_{AABW}}$, is another important factor determining global DIC_{dis}. This varies less significantly than f_{AABW} over the range of simulations, in part due to competing effects of different processes. Surface ocean DIC_{dis} in the Southern Ocean grows in response to upwelling of deepwater, which brings DIC-charged waters to the surface, thus contributing to the carbon supersaturation. Thus, when deep convection is occurring, the rapid injection of carbon to the surface tends to inflate DIC_{dis}. Like the f_{AABW}, ventilation rates (as quantified by global ideal age) are high at both the cold and hot extremes (Galbraith and de Lavergne, submitted), also contributing to the intervening minimum in DIC_{dis} in the AABW formation regions.

Sea ice in the Southern Ocean exerts a further control over DIC_{dis}, as this reduces air-sea gas exchange, thus allowing carbon to accumulate beneath the ice. The total sea ice cover decreases continuously from the low to high CO_2 simulations (fig. 6), but DIC_{dis} is markedly higher in the glacial-like scenarios compared to $CO_2 = 270$ or 911 ppm (fig. 7 and 8). In the glacial state, high DIC_{dis} is a widespread characteristic of the sea surface, whereas in the 270 and 911 ppm simulations, high DIC_{dis}

Biogeosciences Discuss., https://doi.org/10.5194/bg-2017-328
Manuscript under review for journal Biogeosciences
Discussion started: 19 September 2017

only occurs in regions of AABW formation during episodes of deep convection. Terrestrial ice sheets cause an increase in the magnitude of DIC_{dis} both in the Southern Ocean and the North Atlantic. Due to the opposing signs in the two regions, these effects partially compensate each other, but the volumetric dominance of AABW causes its DIC_{dis} increase to win out, raising global DIC_{dis}.

4.4 Disequilibrium O_2

$O_{2_{dis}}$ is also sensitive to sea ice cover, but with a pronounced difference from DIC_{dis}. Because O_2 has a much shorter time scale of exchange at the ocean-atmosphere interface, equilibrating one order of magnitude faster than CO_2, it is not sensitive to sea ice as long as there remains a fair degree of open water (Stephens and Keeling, 2000). But as the sea ice concentration approaches complete coverage, O_2 equilibration rapidly becomes quite sensitive to sea ice. If there is a significant undersaturation of O_2 in upwelling waters, the disequilibrium can become quite large (fig. 9).

In the model simulations, the magnitude of $O_{2_{dis}}$ in the Southern Ocean is as high as 100 μmol/kg. Because the disequilibrium depends on the O_2 depletion of waters upwelling at the Southern Ocean surface, it could potentially be even higher, if upwelling waters had lower O_2. This suggests the hypothesis that very extensive sea ice cover over most of the exposure pathway in the Southern Ocean might have made a significant contribution to the low O_2 concentrations reconstructed for the glacial (Jaccard et al., 2016; Lu et al., 2015).

4.5 Iron fertilization-driven changes in DIC_{soft} and DIC_{dis}

As expected, both the global export and DIC_{soft} increase when dust deposition is increased. However, the DIC_{soft} increase is significantly lower in the well-ventilated glacial-like simulations (2.9 μmol/kg) compared to the interglacial-like simulation (7.3 μmol/kg). This difference is qualitatively in accordance with the age multiplied by export relationship (fig. 3), though with a smaller increase of DIC_{soft} than would be expected from the export increase, compared to the broad spectrum of climate-driven changes. This reduced sensitivity to export can be attributed to the fact that the iron-enhanced export occurs in the Southern Ocean, where the remineralized carbon can be quickly returned to the surface by upwelling when ventilation is strong. Thus, the impact of iron fertilization on DIC_{soft} is strongly dependent on Southern Ocean circulation.

The iron addition also causes an increase of DIC_{dis}, of approximately equal magnitude to DIC_{soft} in the interglacial-like simulation, and of relatively greater proportion in the glacial-like simulations. Because the ocean in the glacial-like simulations is strongly ventilated, with extensive sea ice cover in the Southern Ocean, the increase in export leads to an increase of DIC_{dis}, as remineralized DIC_{soft} is rapidly returned to the Southern Ocean surface, where it has a relatively short residence time and the extensive sea ice inhibits outgassing to the atmosphere. Thus, with rapid Southern Ocean circulation and extensive sea ice cover, a good deal of the DIC sequestered by iron fertilization ends up in the form of DIC_{dis}, rather than DIC_{soft} as frequently assumed. Furthermore, experiments in which the remineralization rate was reduced by 25% indicate that the effects of iron fertilization alone on both DIC_{soft} and DIC_{dis} are quite insensitive to the remineralization rate (see fig. 2) Thus, the effects of iron fertilization and changes in the remineralization rate can be well-approximated as being linearly additive.

Biogeosciences Discuss., https://doi.org/10.5194/bg-2017-328
Manuscript under review for journal Biogeosciences
Discussion started: 19 September 2017

The tendency to sequester carbon as DIC_{dis} vs. DIC_{soft} can be quantified by the global ratio $\Delta DIC_{dis}/\Delta DIC_{soft}$. Our experiments suggest that this ratio is 0.9 for the pre-industrial state and 3.3 for the glacial-like state. Because of the circulation dependence of this ratio, it is expected that there could be significant variation between models. It is worth noting that Parekh et al. (2006) found $\Delta DIC_{dis}/\Delta DIC_{soft}$ of 2 in response to iron fertilization, using a modern ocean circulation, as analyzed by Ito and Follows (2013). We also caution that the quantitative values of DIC_{soft} and DIC_{dis} resulting from the altered iron flux should be taken with a grain of salt, given the very large uncertainty in models of iron cycling (Tagliabue et al., 2016).

4.6 A unified framework for DIC_{dis} and preformed nutrients

The concept of preformed nutrients allowed the production of a very useful body of work, striving for simple predictive principles. This work highlighted the importance of the nutrient concentrations in polar oceans where deep waters form (Sigman and Boyle, 2000; Ito and Follows, 2005; Marinov et al., 2008a) as well as changes in the ventilation fractions of AABW and NADW, given their very different preformed nutrient concentrations (Schmittner and Galbraith, 2008; Marinov et al., 2008b). Although the variability of P:C ratios implies significant uncertainty for the utility of $PO4_{pre}$ in the ocean, the relative constancy of N:C ratios suggests that $NO3_{pre}$ is indeed linked to DIC_{soft}, inasmuch as the global N inventory is fixed (Galbraith and Martiny, 2015).

However, as shown by the analyses here, DIC_{soft} – reflected by the preformed nutrients – is only half the story. Changes in DIC_{dis} can be of equivalent magnitude, and can vary independently of DIC_{soft} as a result of changes in ocean circulation and sea ice. Nonetheless, we find that the same conceptual approach developed for DIC_{soft} can be used to predict DIC_{dis} from the end member DIC_{dis} and the global volume fractions. The preformed relationships and DIC_{dis} can therefore be unified as follows (see fig. 10):

$$DIC_{soft} = NO3_{rem} \cdot r_{C:N} \tag{8}$$

Remineralized nitrate can be expressed in terms of the global nitrate inventory and the accumulated nitrate loss due to pelagic and benthic denitrification, analagous to AOU:

$$NO3_{rem} = NO3_{global} - NO3_{pre} + NO3_{den} \tag{9}$$

$$NO3_{pre} \approx f_{SO} \cdot NO3_{pre_{SO}} + f_{NAtl} \cdot NO3_{pre_{NAtl}} + f_{NPac} \cdot NO3_{pre_{NPac}} \tag{10}$$

Above, for simplicity, we consider only the deep ocean DIC_{dis}. Now, however, we would like to include the upper ocean (above 1 km) as well. Because there is production of intermediate water but no deep convection in the North Pacific, we calculate this mass balance for the upper ocean (above 1 km) and deep ocean separately, dropping the final term in Eq. 10 in the calculation below 1 km:

$$DIC_{soft_{deep}} \approx r_{C:N} \cdot [NO3_{deep} + NO3_{den,deep} - (f_{SO,deep} \cdot NO3_{pre_{SO,deep}} + f_{NAtl,deep} \cdot NO3_{pre_{NAtl,deep}})] \tag{11}$$

Biogeosciences Discuss., https://doi.org/10.5194/bg-2017-328
Manuscript under review for journal Biogeosciences
Discussion started: 19 September 2017

The same calculations, including the North Pacific component, are performed to obtain $\mathrm{DIC}_{\mathrm{soft}_{\mathrm{upper}}} + \mathrm{DIC}_{\mathrm{dis}_{\mathrm{upper}}}$; here we expand only the deep ocean component for simplicity.

$$\begin{aligned}\mathrm{DIC}_{\mathrm{dis}_{\mathrm{deep}}} + \mathrm{DIC}_{\mathrm{soft}_{\mathrm{deep}}} \approx & r_{\mathrm{C:N}} \cdot (\mathrm{NO}_{3_{\mathrm{deep}}} + \mathrm{NO}_{3_{\mathrm{den,deep}}}) + f_{\mathrm{SO,deep}} \cdot (\mathrm{DIC}_{\mathrm{dis}_{\mathrm{SO,deep}}} - r_{\mathrm{C:N}} \cdot \mathrm{NO}_{3_{\mathrm{pre}_{\mathrm{SO,deep}}}}) \\ & + f_{\mathrm{NAtl,deep}} \cdot (\mathrm{DIC}_{\mathrm{dis}_{\mathrm{NAtl,deep}}} - r_{\mathrm{C:N}} \cdot \mathrm{NO}_{3_{\mathrm{pre}_{\mathrm{NAtl,deep}}}}) \end{aligned} \tag{12}$$

Finally, the global average is computed by summing the volume-weighted values in the upper and deep ocean:

$$\mathrm{DIC}_{\mathrm{dis}_{\mathrm{global}}} + \mathrm{DIC}_{\mathrm{soft}_{\mathrm{global}}} \approx [V_{\mathrm{upper}} \cdot (\mathrm{DIC}_{\mathrm{dis}_{\mathrm{upper}}} + \mathrm{DIC}_{\mathrm{soft}_{\mathrm{upper}}}) + V_{\mathrm{deep}} \cdot (\mathrm{DIC}_{\mathrm{dis}_{\mathrm{deep}}} + \mathrm{DIC}_{\mathrm{soft}_{\mathrm{deep}}})]/V_{\mathrm{total}} \tag{13}$$

Fully expanded, this yields:

$$\begin{aligned}\mathrm{DIC}_{\mathrm{dis}_{\mathrm{global}}} + \mathrm{DIC}_{\mathrm{soft}_{\mathrm{global}}} \approx & \frac{V_{\mathrm{upper}}}{V_{\mathrm{total}}} [r_{\mathrm{C:N}} \cdot (\mathrm{NO}_{3_{\mathrm{upper}}} + \mathrm{NO}_{3_{\mathrm{den,upper}}}) + f_{\mathrm{SO,upper}} \cdot (\mathrm{DIC}_{\mathrm{dis}_{\mathrm{SO,upper}}} - r_{\mathrm{C:N}} \cdot \mathrm{NO}_{3_{\mathrm{pre}_{\mathrm{SO,upper}}}}) \\ & + f_{\mathrm{NAtl,upper}} \cdot (\mathrm{DIC}_{\mathrm{dis}_{\mathrm{NAtl,upper}}} - r_{\mathrm{C:N}} \cdot \mathrm{NO}_{3_{\mathrm{pre}_{\mathrm{NAtl,upper}}}})] \\ & + \frac{V_{\mathrm{deep}}}{V_{\mathrm{total}}} [r_{\mathrm{C:N}} \cdot (\mathrm{NO}_{3_{\mathrm{deep}}} + \mathrm{NO}_{3_{\mathrm{den,deep}}}) + f_{\mathrm{SO,deep}} \cdot (\mathrm{DIC}_{\mathrm{dis}_{\mathrm{SO,deep}}} - r_{\mathrm{C:N}} \cdot \mathrm{NO}_{3_{\mathrm{pre}_{\mathrm{SO,deep}}}}) \\ & + f_{\mathrm{NAtl,deep}} \cdot (\mathrm{DIC}_{\mathrm{dis}_{\mathrm{NAtl,deep}}} - r_{\mathrm{C:N}} \cdot \mathrm{NO}_{3_{\mathrm{pre}_{\mathrm{NAtl,deep}}}})] \end{aligned} \tag{14}$$

which can be generalized for any number n of ventilation regions i as:

$$\mathrm{DIC}_{\mathrm{dis}_{\mathrm{global}}} + \mathrm{DIC}_{\mathrm{soft}_{\mathrm{global}}} \approx r_{\mathrm{C:N}} \cdot (\mathrm{NO}_{3_{\mathrm{global}}} + \mathrm{NO}_{3_{\mathrm{den,global}}}) + \sum_{i=1}^{n} f_i \cdot (\mathrm{DIC}_{\mathrm{dis}_i} - r_{\mathrm{C:N}} \cdot \mathrm{NO}_{3_{\mathrm{pre}_i}}) \tag{15}$$

Thus, total carbon storage as soft and disequilibrium carbon (i.e. everything other than $\mathrm{DIC}_{\mathrm{sat}}$ and $\mathrm{DIC}_{\mathrm{carb}}$) varies with the global nitrate inventory, corrected for NO_3 loss to denitrification, and the difference between $\mathrm{DIC}_{\mathrm{dis}}$ and $r_{\mathrm{C:N}} \cdot \mathrm{NO}_{3_{\mathrm{pre}}}$ in the polar oceans, modulated by their respective volume fractions. It is interesting that this relationship is more accurate than either $\mathrm{DIC}_{\mathrm{dis}}$ or $\mathrm{DIC}_{\mathrm{soft}}$, among our suite of simulations, with an RMSE of 3.6, 7.0 and 5.2 μmol kg^{-1} for $\mathrm{DIC}_{\mathrm{dis}} + \mathrm{DIC}_{\mathrm{soft}}$, $\mathrm{DIC}_{\mathrm{dis}}$ and $\mathrm{DIC}_{\mathrm{soft}}$, respectively.

4.7 $\mathrm{DIC}_{\mathrm{dis}}$ nadir and peak CO_2

The model simulations show a clear minimum of $\mathrm{DIC}_{\mathrm{dis}}$ at intermediate CO_2 (270 – 405 ppm). As we have shown, this occurs as a result of the minimum contribution of AABW to the global ocean, and to a lesser extent, a minimum in the $\mathrm{DIC}_{\mathrm{dis}}$ of AABW. It is important to note that $\mathrm{DIC}_{\mathrm{dis}}$ is not just a function of ocean circulation, soft tissue pump and sea ice, which are simulated here, but also the CO_2 driving gas exchange due to its impacts on saturation CO_2^* and $\mathrm{DIC}_{\mathrm{sat}}$, which here is held fixed at 270 ppm. Because $\mathrm{DIC}_{\mathrm{dis}}$ is calculated as the departure from equilibrium with atmospheric CO_2 at 270 ppm, we expect that the resulting changes in $\mathrm{DIC}_{\mathrm{dis}}$ under interactive CO_2 will differ only due to minor, non-linear effects. So, although this simplification (in combination with other model biases) prevents a strict interpretation of the CO_2 and orbital combination at which this nadir is likely to occur, its robust emergence from the relative density control on deep water ventilation volumes makes its existence appear reasonable (Galbraith and de Lavergne, submitted).

Biogeosciences Discuss., https://doi.org/10.5194/bg-2017-328
Manuscript under review for journal Biogeosciences
Discussion started: 19 September 2017

A minimum global extent of AABW during interglacials has been documented from ϵ_{Nd} (Piotrowski et al., 2005), and it has been shown that AABW likely ceased to form entirely for a brief portion of the last interglacial, marine isotope stage 5e (Hayes et al., 2014). We suggest that the minimum AABW extent produced a nadir of DIC_{dis} that may have contributed to a "soft" upper limit on CO_2 during interglacials. Galbraith and Eggleston (2017) showed that the lower limit of CO_2 over glacial cycles is quite firm and that low CO_2 is very common. In addition, they showed that, although the peak values of CO_2 during interglacials vary significantly, interglacial CO_2 levels are relatively common, suggesting that they are also a preferred state. We propose that the DIC_{dis} nadir would have contributed to preventing a significant CO_2 rise above interglacial CO_2, since a rise of temperatures above that which gives the DIC_{dis} nadir will increase AABW formation and thereby draw down CO_2 as DIC_{dis}. Of course this would be counteracted by an increase of DIC_{soft}, if it were to behave opposite of DIC_{dis}, as occurs in our simulations – whether or not this is true depends on unresolved climate dependencies in the marine ecosystem, which currently remains an open question. We do not claim that this soft upper limit was significant, but simply propose the possibility as a hypothesis that can be tested.

5 Conclusions

Carbon storage in the ocean can be quantified as the sum of the saturation, soft tissue, carbonate, and disequilibrium components. Our simulations indicate that the latter may play a very important role, which has been largely neglected in other studies. Changes in the climate state tend to drive the soft tissue pump and the disequilibrium pump in opposite directions. However, this is not necessarily true in the real ocean, given that the simulated anticorrelation is not mechanistically required, but instead arises from the fact that f_{AABW} and ideal age · export are anticorrelated in the simulations. There is plenty of scope for these to have varied in additional ways, not captured by our idealized simulations.

Iron fertilization experiments are a popular method of testing the sensitivity of pCO_2 to an increase in dust flux to the Southern Ocean; here, these simulations illustrate the non-linearity of the effects of circulation and increased primary productivity on DIC. At moderate ventilation rates (the pre-industrial control run), an increase in iron results in an increase both in DIC_{soft}, due to higher biological export, and DIC_{dis}, because of the upwelling of C-rich water resulting from higher remineralization. However, under a "glacial" state, high ventilation in this model produces only a small increase in DIC_{soft} in response to increased Fe in the surface ocean, as the remineralized carbon is quickly returned to the surface, thus producing a significant increase in DIC_{dis} only. This also raises an important warning for iron fertilization studies: the CO_2 impact of Southern Ocean iron addition can actually be dominated by the DIC_{dis}, so that the overall impact may be significantly larger than would be predicted from DIC_{soft} and/or O_2 utilization.

The results presented here suggest that disequilibrium carbon should be considered as a major component of ocean carbon storage, linked to ocean circulation, sea ice and biological export in non-linear and interdepenent ways. Despite these non-linearities, we suggest that the resulting global carbon storage can be well-approximated by a simple relationship including the global nitrate inventory, and the DIC_{dis} and preformed CO_3 in ocean ventilation regions (eq. 15). The glacial simulations suggest that disequilibrium carbon may have been the dominant component of oceanic carbon uptake during cold phases of

Biogeosciences Discuss., https://doi.org/10.5194/bg-2017-328
Manuscript under review for journal Biogeosciences
Discussion started: 19 September 2017

the ice age cycles. As this study represents the result of a single model, prone to bias, it would be very useful to test our results using other GCMs. It would also be useful to consider how disequilibrium carbon can change under future pCO_2 levels, including developing observational constraints on its past and present magnitude, and exploring the degree to which inter-model variations in DIC_{dis} may contribute to uncertainty in climate projections.

Code availability. Code is available on request; please contact E. D. Galbraith (eric.galbraith@icrea.cat).

Appendix A: DIC decomposition

DIC is treated as the sum of four components:

$$\mathrm{DIC} = \mathrm{DIC_{sat}} + \mathrm{DIC_{dis}} + \mathrm{DIC_{soft}} + \mathrm{DIC_{carb}} \tag{A1}$$

$\mathrm{DIC_{sat}}$ is the DIC at equilibrium with the atmosphere given the surface ocean temperature, salinity, and alkalinity and the atmospheric pCO_2 calculated following Zeebe and Wolf-Gladrow (2001):

$$\mathrm{DIC_{sat}} = f(\mathrm{T}, \mathrm{S}, \mathrm{alk_{pre}}, pCO_2) \tag{A2}$$

In this model, $\mathrm{DIC_{soft}}$ is proportional to the utilized O_2, which is defined as the difference between preformed and total O_2, where the ratio of remineralized C to O_2 ($r_{C:O_2}$) is 106:150.

$$\mathrm{DIC_{soft}} = r_{\mathrm{C:O_2}} \cdot (\mathrm{O_{2_{pre}}} - \mathrm{O_2}) \tag{A3}$$

DIC derived from $CaCO_3$ dissolution is proportional to the change in alkalinity, correcting for the additional change in alkalinity due to hydrogen ion addition during organic matter remineralization.

$$\mathrm{DIC_{carb}} = 0.5 \cdot [(\mathrm{alk} - \mathrm{alk_{pre}}) + r_{\mathrm{N:O_2}} \cdot (\mathrm{O_{2_{pre}}} - \mathrm{O_2})] \tag{A4}$$

Preformed alkalinity, defined as the total alkalinity at the surface and treated as a conservative tracer, was reconstructed here annually through multilinear regressions as a function of century-averaged salinity (S), temperature (T), and preformed O_2, NO_3^- and PO_4^{3-}.

$$\begin{aligned}\mathrm{alk_{pre}} =& (a_0 + a_1 \cdot \mathrm{S}' + a_2 \cdot \mathrm{T}' + a_3 \cdot \mathrm{O_{2_{pre}}} + a_4 \cdot \mathrm{NO_{3_{pre}}} + a_5 \cdot \mathrm{PO_{4_{pre}}}) \cdot \mathrm{NAtl} \\ &+ (b_0 + b_1 \cdot \mathrm{S}' + b_2 \cdot \mathrm{T}' + b_3 \cdot \mathrm{O_{2_{pre}}} + b_4 \cdot \mathrm{NO_{3_{pre}}} + b_5 \cdot \mathrm{PO_{4_{pre}}}) \cdot \mathrm{SO} \\ &+ (c_0 + c_1 \cdot \mathrm{S}' + c_2 \cdot \mathrm{T}' + c_3 \cdot \mathrm{O_{2_{pre}}} + c_4 \cdot \mathrm{NO_{3_{pre}}} + c_5 \cdot \mathrm{PO_{4_{pre}}}) \cdot (1 - \mathrm{SO} - \mathrm{NAtl})\end{aligned} \tag{A5}$$

where $\mathrm{S}' = \mathrm{S} - 35$, $\mathrm{T}' = \mathrm{T} - 20^{\circ}\mathrm{C}$, the a_i are determined by a regression in the surface North Atlantic, the b_i for the SO, and the c_i using the model output elsewhere in the surface. The tracers SO and NAtl are set to 1 in the surface Southern Ocean (south of 30°S) and the North Atlantic (north of 30°N), respectively, and are conservatively mixed into the ocean interior. This

parametrization induces an uncertainty on the order of 1 μmol/kg in globally averaged DIC_{dis} (see fig. 11). As discussed above, however, this is small compared to the signal seen over all simulations.

Finally, DIC_{dis} has been back-calculated from the model output as a residual.

$$DIC_{dis} = DIC - DIC_{sat} - DIC_{soft} - DIC_{carb} \quad \text{(A6)}$$

Author contributions. E. D. Galbraith conducted the model simulations, S. Eggleston performed the analysis, and both contributed to writing the manuscript.

Competing interests. The authors declare that they have no conflict of interest.

Acknowledgements. The authors would like to thank R. Bernardello for very helpful discussion. S. Eggleston is funded by a fellowship from the Swiss National Science Foundation. E. D. Galbraith acknowledges computing support from the Canadian Foundation for Innovation and Compute Canada, and financial support from the Spanish Ministry of Economy and Competitiveness, through the María de Maeztu Programme for Centres/Units of Excellence in R&D (MDM-2015-0552).

References

Bernardello, R., Marinov, I., Palter, J. B., Sarmiento, J. L., Galbraith, E. D., and Slater, R. D.: Response of the Ocean Natural Carbon Storage to Projected Twenty-First-Century Climate Change, J. Climate, 27, 2033–2053, doi:10.1175/jcli-d-13-00343.1, 2014.

Broecker, W. S. and Peng, T.-H.: Gas exchange rates between air and sea, Tellus, 26, 21–35, 1974.

Duteil, O., Koeve, W., Oschlies, A., Bianchi, D., Galbraith, E., Kriest, I., and Matear, R.: A novel estimate of ocean oxygen utilisation points to a reduced rate of respiration in the ocean interior, Biogeosciences, 10, 7723–7738, doi:10.5194/bg-10-7723-2013, 2013.

François, R., Altabet, M. A., Yu, E.-F., Sigman, D. M., Bacon, M. P., Frank, M., Bohrmann, G., Bareille, G., and Labeyrie, L. D.: Contribution of Southern Ocean surface-water stratification to low atmospheric CO_2 concentrations during the last glacial period, Nature, 389, 929–935, doi:10.1038/40073, 1997.

Galbraith, E. D. and Eggleston, S.: A lower limit to atmospheric CO_2 concentrations over the past 800,000 years, Nat. Geosci., 10, 295–298, doi:10.1038/ngeo2914, 2017.

Galbraith, E. D. and Martiny, A. C.: A simple nutrient-dependent mechanism for predicting the stoichiometry of marine ecosystems, P. Natl. Acad. Sci. USA, 112, 8199–8204, doi:10.1073/pnas.1423917112, 2015.

Galbraith, E. D., Gnanadesikan, A., Dunne, J. P., and Hiscock, M. R.: Regional impacts of iron-light colimitation in a global biogeochemical model, Biogeosciences, 7, 1043–1064, doi:10.5194/bg-7-1043-2010, 2010.

Galbraith, E. D., Kwon, E. Y., Gnanadesikan, A., Rodgers, K. B., Griffies, S. M., Bianchi, D., Sarmiento, J. L., Dunne, J. P., Simeon, J., Slater, R. D., Wittenberg, A. T., and Held, I. M.: Climate Variability and Radiocarbon in the CM2Mc Earth System Model, J. Climate, 24, 4230–4254, doi:10.1175/2011jcli3919.1, 2011.

Gebbie, G. and Huybers, P.: How is the ocean filled?, Geophys. Res. Lett., 38, doi:10.1029/2011gl046769, 2011.

Goodwin, P., Follows, M. J., and Williams, R. G.: Analytical relationships between atmospheric carbon dioxide, carbon emissions, and ocean processes, Global Biogeochem. Cy., 22, doi:10.1029/2008gb003184, 2008.

Hayes, C. T., Martínez-García, A., Hasenfratz, A. P., Jaccard, S. L., Hodell, D. A., Sigman, D. M., Haug, G. H., and Anderson, R. F.: A stagnation event in the deep South Atlantic during the last interglacial period, Science, 346, 1514–1517, doi:10.1126/science.1256620, 2014.

IPCC: Climate Change 2007: The Physical Science Basis. Contribution of Working Group I to the Fourth Assessment Report of the Intergovernmental Panel on Climate Change, Cambridge University Press, Cambridge, United Kingdom, 2007.

Ito, T. and Follows, M. J.: Preformed phosphate, soft tissue pump and atmospheric CO_2, J. Mar. Res., 63, 813–839, doi:10.1357/0022240054663231, 2005.

Ito, T. and Follows, M. J.: Air-sea disequilibrium of carbon dioxide enhances the biological carbon sequestration in the Southern Ocean, Global Biogeochem. Cy., 27, 1129–1138, doi:10.1002/2013gb004682, 2013.

Ito, T., Follows, M. J., and Boyle, E. A.: Is AOU a good measure of respiration in the oceans?, Geophys. Res. Lett., 31, doi:10.1029/2004GL020900, 2004.

Jaccard, S. L., Galbraith, E. D., Martínez-García, A., and Anderson, R. F.: Covariation of deep Southern Ocean oxygen and atmospheric CO_2 through the last ice age, Nature, 530, 207–210, doi:10.1038/nature16514, 2016.

Kohfeld, K. E. and Ridgwell, A.: Glacial-interglacial variability in atmospheric CO_2, Geophysical Monograph Series, pp. 251–286, doi:10.1029/2008gm000845, 2009.

Kwon, E. Y., Primeau, F., and Sarmiento, J. L.: The impact of remineralization depth on the air-sea carbon balance, Nat. Geosci., 2, 630–635, doi:10.1038/NGEO612, 2009.

Laskar, J., Robutel, P., Joutel, F., Gastineau, M., Correia, A. C. M., and Levrard, B.: A long-term numerical solution for the insolation quantities of the Earth, Astron. Astrophys., 428, 261–285, doi:10.1051/0004-6361:20041335, 2004.

Lu, Z., Hoogakker, B. A. A., Hillenbrand, C.-D., Zhou, X., Thomas, E., Gutchess, K. M., Lu, W., Jones, L., and Rickaby, R. E. M.: Oxygen depletion recorded in upper waters of the glacial Southern Ocean, Nat. Commun., 7, doi:10.1038/ncomms11146, 2015.

Marinov, I., Follows, M., Gnanadesikan, A., Sarmiento, J. L., and Slater, R. D.: How does ocean biology affect atmospheric pCO_2? Theory and models, J. Geophys. Res., 113, doi:10.1029/2007jc004598, 2008a.

Marinov, I., Gnanadesikan, A., Sarmiento, J. L., Toggweiler, J. R., Follows, M., and Mignone, B. K.: Impact of oceanic circulation on biological carbon storage in the ocean and atmospheric pCO_2, Global Biogeochem. Cy., 22, doi:10.1029/2007gb002958, 2008b.

Martin, J. H.: Glacial-interglacial CO_2 change: The Iron Hypothesis, Paleoceanography, 5, 1–13, doi:10.1029/pa005i001p00001, 1990.

Martin, J. H., Knauer, G. A., Karl, D. M., and Broenkow, W. W.: VERTEX: carbon cycling in the northeast Pacific, Deep-Sea Res. A, 34, 267–285, doi:10.1016/0198-0149(87)90086-0, 1987.

Martiny, A. C., Vrugt, J. A., Primeau, F. W., and Lomas, M. W.: Regional variation in the particulate organic carbon to nitrogen ratio in the surface ocean, Global Biogeochem. Cy., 27, 723–731, doi:10.1002/gbc.20061, 2013.

Matsumoto, K., Hashioka, T., and Yamanaka, Y.: Effect of temperature-dependent organic carbon decay on atmospheric pCO_2, J. Geophys. Res., 112, doi:10.1029/2006JG000187, 2007.

Nickelsen, L. and Oschlies, A.: Enhanced sensitivity of oceanic CO_2 uptake to dust deposition by iron-light colimitation, Geophys. Res. Lett., 42, 492–499, doi:10.1002/2014gl062969, 2015.

Parekh, P., Dutkiewicz, S., Follows, M. J., and Ito, T.: Atmospheric carbon dioxide in a less dusty world, Geophys. Res. Lett., 33, doi:10.1029/2005gl025098, 2006.

Piotrowski, A. M., Goldstein, S. L., Hemming, S. R., and Fairbanks, R. G.: Temporal Relationships of Carbon Cycling and Ocean Circulation at Glacial Boundaries, Science, 307, 1933–1938, doi:10.1126/science.1104883, 2005.

Roth, R., Ritz, S. P., and Joos, F.: Burial-nutrient feedbacks amplify the sensitivity of atmospheric carbon dioxide to changes in organic matter remineralisation, Earth System Dynamics, 5, 321–343, doi:10.5194/esd-5-321-2014, 2014.

Schmittner, A. and Galbraith, E. D.: Glacial greenhouse-gas fluctuations controlled by ocean circulation changes, Nature, 456, 373–376, doi:10.1038/nature07531, 2008.

Sigman, D. M. and Boyle, E. A.: Glacial/interglacial variations in atmospheric carbon dioxide, Nature, 407, 859–869, doi:10.1038/35038000, http://dx.doi.org/10.1038/35038000, 2000.

Sigman, D. M., Hain, M. P., and Haug, G. H.: The polar ocean and glacial cycles in atmospheric CO_2 concentration, Nature, 466, 47–55, doi:10.1038/nature09149, 2010.

Skinner, L. C.: Glacial-interglacial atmospheric CO_2 change: a possible "standing volume" effect on deep-ocean carbon sequestration, Clim. Past, 5, 537–550, doi:10.5194/cp-5-537-2009, http://dx.doi.org/10.5194/cp-5-537-2009, 2009.

Stephens, B. B. and Keeling, R. F.: The influence of Antarctic sea ice on glacial-interglacial CO_2 variations, Nature, 404, 171–174, doi:10.1038/35004556, 2000.

Tagliabue, A., Aumont, O., DeAth, R., Dunne, J. P., Dutkiewicz, S., Galbraith, E., Misumi, K., Moore, J. K., Ridgwell, A., Sherman, E., Stock, C., Vichi, M., Völker, C., and Yool, A.: How well do global ocean biogeochemistry models simulate dissolved iron distributions?, Global Biogeochem. Cy., 30, 149–174, doi:10.1002/2015GB005289, 2016.

Takahashi, T. Sutherland, S. C., Wanninkhof, R., Sweeney, C., Feely, R. A., Chipman, D. W., Hales, B., Friederich, G., Chavez, F., Watson, A., Bakker, D. C. E., Schuster, U., Metzl, N., Yoshikawa-Inoue, H., Ishii, M., Midorikawa, T., Nojiri, Y., Sabine, C., Olafsson, J., Arnarson, T. S., Tilbrook, B., Johannessen, T., Olsen, A., Bellerby, R., Körtzinger, A., Steinhoff, T., Hoppema, M., de Baar, H. J. W., Wong, C. S., Delille, B., and Bates, N. R.: Climatological mean and decadal changes in surface ocean pCO_2, and net sea-air CO_2 flux over the global oceans, Deep-Sea Res. II, 56, 554–577, doi:10.1016/j.dsr2.2008.12.009, 2009.

Toggweiler, J. R., Murnane, R., Carson, S., Gnanadesikan, A., and Sarmiento, J. L.: Representation of the carbon cycle in box models and GCMs: 2. Organic pump, Global Biogeochem. Cy., 17, doi:10.1029/2001gb001841, 2003.

Tschumi, T., Joos, F., Gehlen, M., and Heinze, C.: Deep ocean ventilation, carbon isotopes, marine sedimentation and the deglacial CO_2 rise, Clim. Past, 7, 771–800, doi:10.5194/cp-7-771-2011, 2011.

Zeebe, R. E. and Wolf-Gladrow, D.: CO_2 in Seawater: Equilibrium, Kinetics, Isotopes, vol. 65, Elsevier Oceanography Series, Amsterdam, 2001.

Biogeosciences Discuss., https://doi.org/10.5194/bg-2017-328
Manuscript under review for journal Biogeosciences
Discussion started: 19 September 2017

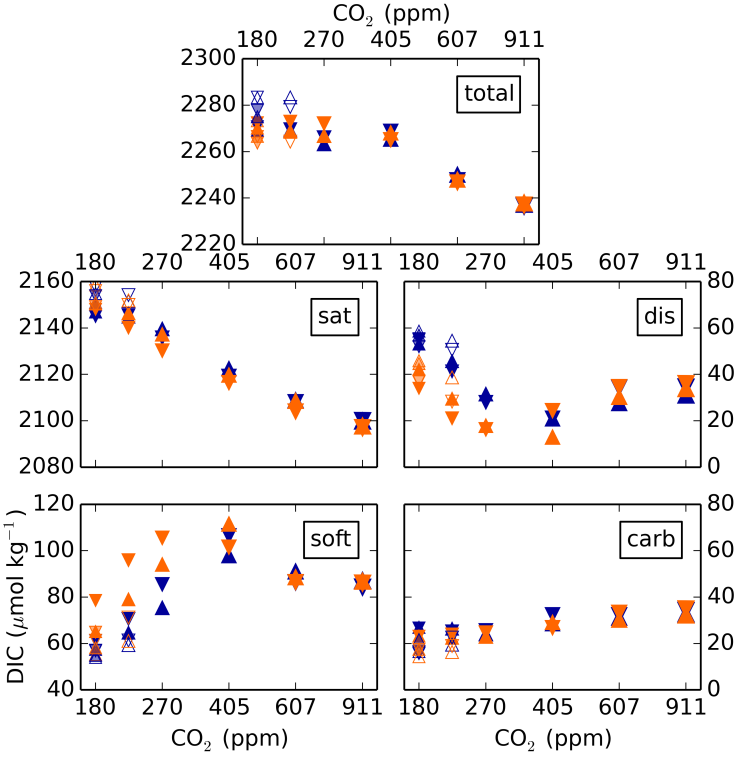

Figure 1. Global average DIC and separate components in simulations 1-36 as a function of CO_2. Orange and blue represent high and low obliquity scenarios, respectively; triangles pointing upward and downward represent greater northern and southern hemisphere seasonality, respectively; outlines are scenarios with LGM ice sheets; light shading indicates scenarios with LGM ice sheet topography but PI albedo.

Biogeosciences Discuss., https://doi.org/10.5194/bg-2017-328
Manuscript under review for journal Biogeosciences
Discussion started: 19 September 2017

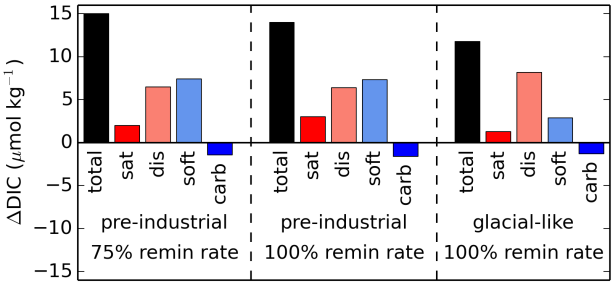

Figure 2. Changes in total global average DIC and each of the components (iron fertilization simulation minus associated control run). Simulations were either run under pre-industrial or glacial-like conditions (in the case of the latter, results represent the average of four runs at $CO_2 = 180$ ppm with LGM ice sheets), as well as 100% and 75% of the default remineralization rate of organic matter. The close agreement of the left and middle panels indicates that the effects of iron fertilization and changes in the remineralization rate are linearly additive in this model.

Biogeosciences Discuss., https://doi.org/10.5194/bg-2017-328
Manuscript under review for journal Biogeosciences
Discussion started: 19 September 2017

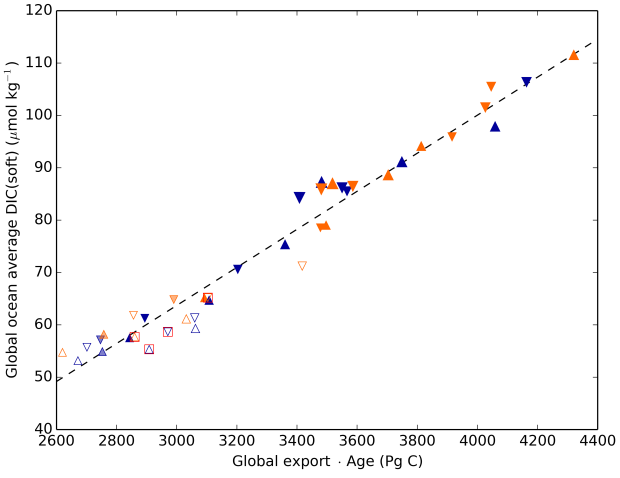

Figure 3. Globally averaged DIC_{soft}, or remineralized carbon from the soft tissue pump, can be approximated remarkably well by the global export flux at 100 m multiplied by the average age of the ocean. The latter is an ideal age tracer in the model that is set to 0 at the surface and ages by 1 y each model year in the ocean interior. Markers as in fig. 1 with the size of the symbols corresponding to the CO_2 level.

Biogeosciences Discuss., https://doi.org/10.5194/bg-2017-328
Manuscript under review for journal Biogeosciences
Discussion started: 19 September 2017

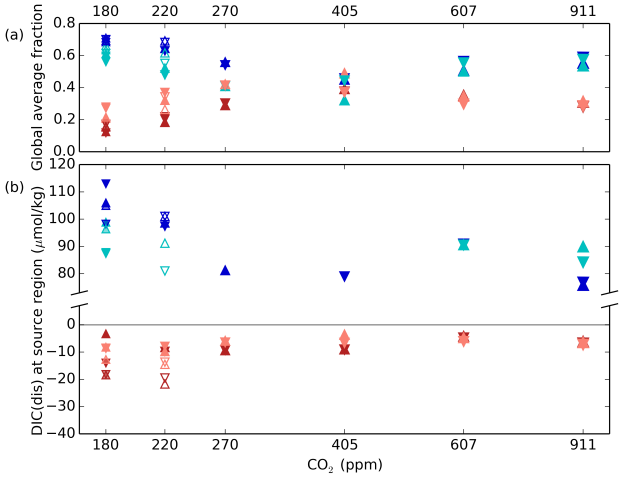

Figure 4. (a) Global average fraction of northern- (reddish colors) and southern-sourced (bluish colors) water. (b) Average values of DIC_{dis} of these water masses determined at 100 m depth in the model where convection down to 200 m occurs. Markers are identical to fig. 1 with lighter colors representing high and darker colors low obliquity.

Biogeosciences Discuss., https://doi.org/10.5194/bg-2017-328
Manuscript under review for journal Biogeosciences
Discussion started: 19 September 2017

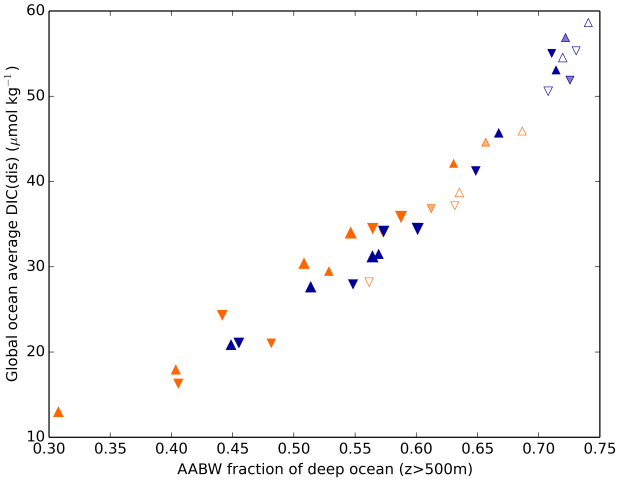

Figure 5. Global average DIC_{dis} as a function of the fraction of the ocean below 500 m derived from the surface Southern Ocean; symbols as in fig. 1 with the size of the symbols corresponding to the CO_2 level.

Biogeosciences Discuss., https://doi.org/10.5194/bg-2017-328
Manuscript under review for journal Biogeosciences
Discussion started: 19 September 2017

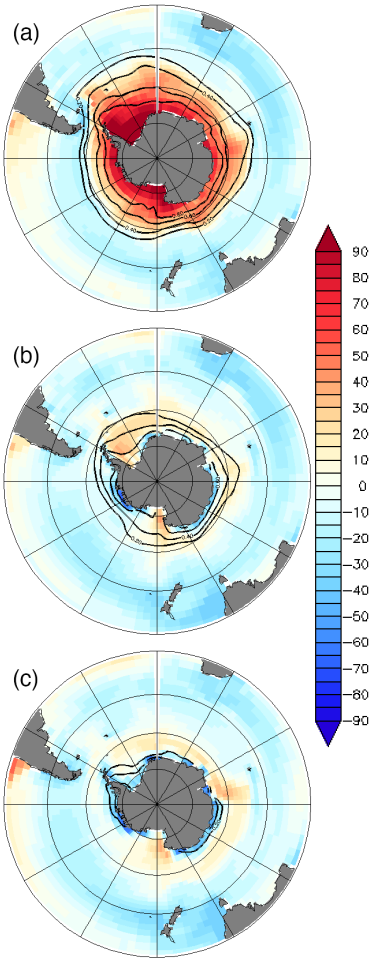

Figure 6. Surface ocean DIC_{dis} and annually averaged sea ice cover (contours showing 20% intervals) in simulations emulating the following states: (a) glacial; (b) interglacial; (c) $CO_2 = 911$.

Biogeosciences Discuss., https://doi.org/10.5194/bg-2017-328
Manuscript under review for journal Biogeosciences
Discussion started: 19 September 2017

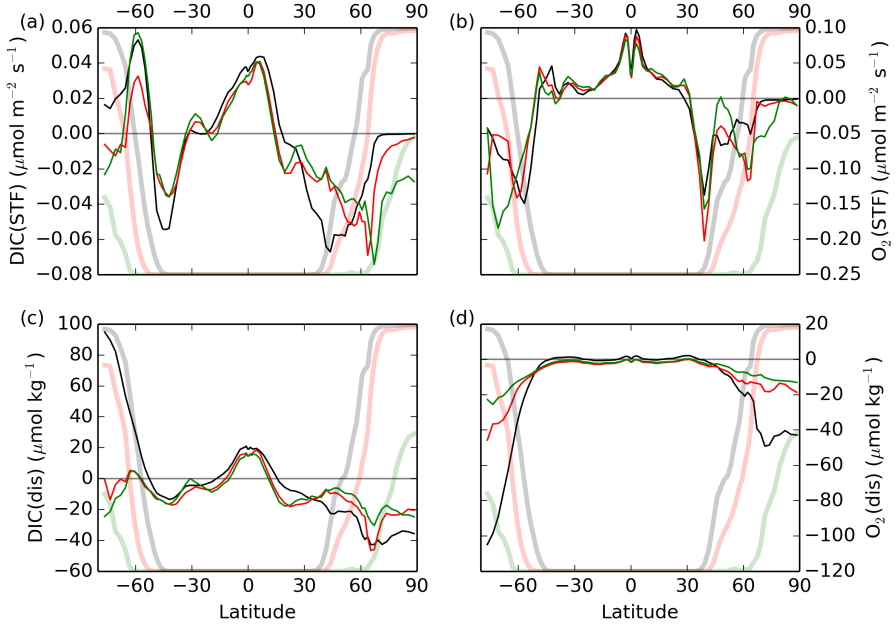

Figure 7. Zonally averaged (a) DIC flux to the atmosphere; (b) O_2 flux to the atmosphere; (c) surface ocean DIC_{dis}; (d) surface ocean $O_{2_{dis}}$. Results from three simulations are shown: glacial (black); interglacial (red); $CO_2 = 911$ (green). Fractional sea ice cover (0 - 100%) is shown in each plot as a reference.

Biogeosciences Discuss., https://doi.org/10.5194/bg-2017-328
Manuscript under review for journal Biogeosciences
Discussion started: 19 September 2017

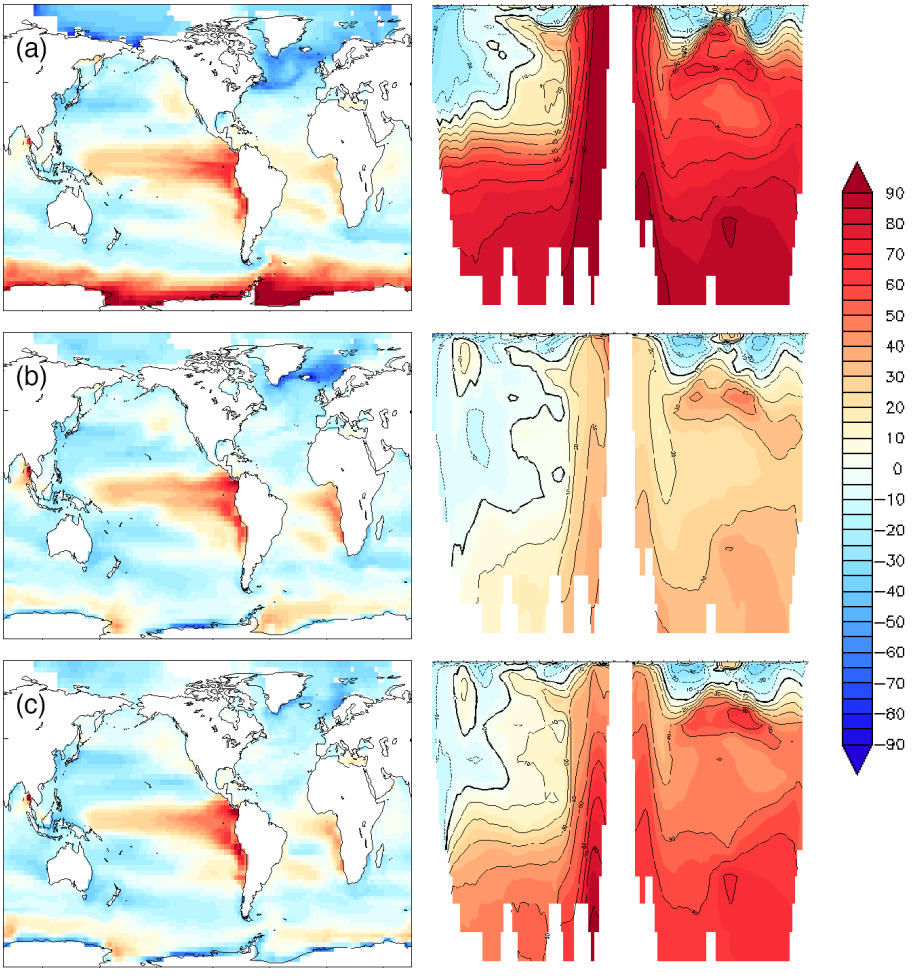

Figure 8. DIC_{dis} (μmol kg^{-1}) for simulations (a) glacial; (b) interglacial; (c) $CO_2 = 911$. Depth transects represent the North Atlantic (left) - Southern Ocean (center) - North Pacific (right).

Biogeosciences Discuss., https://doi.org/10.5194/bg-2017-328
Manuscript under review for journal Biogeosciences
Discussion started: 19 September 2017

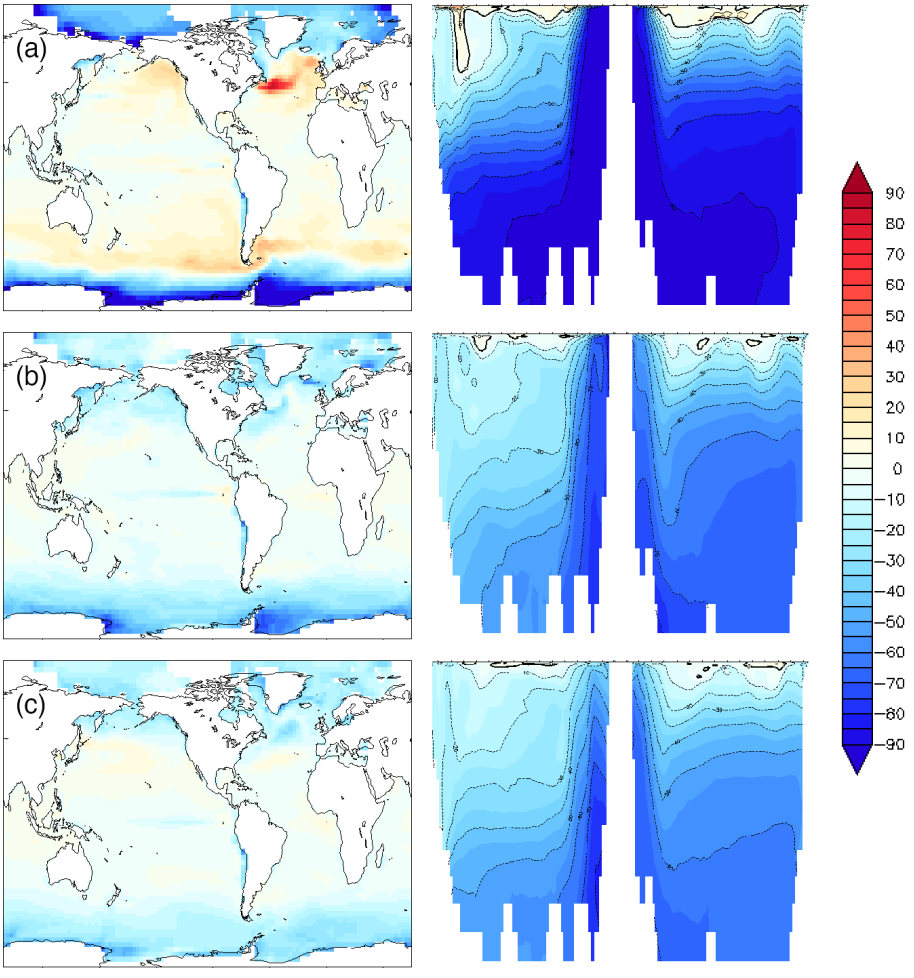

Figure 9. As in fig. 8 for $O_{2_{dis}}$ (μmol kg^{-1})

Biogeosciences Discuss., https://doi.org/10.5194/bg-2017-328
Manuscript under review for journal Biogeosciences
Discussion started: 19 September 2017

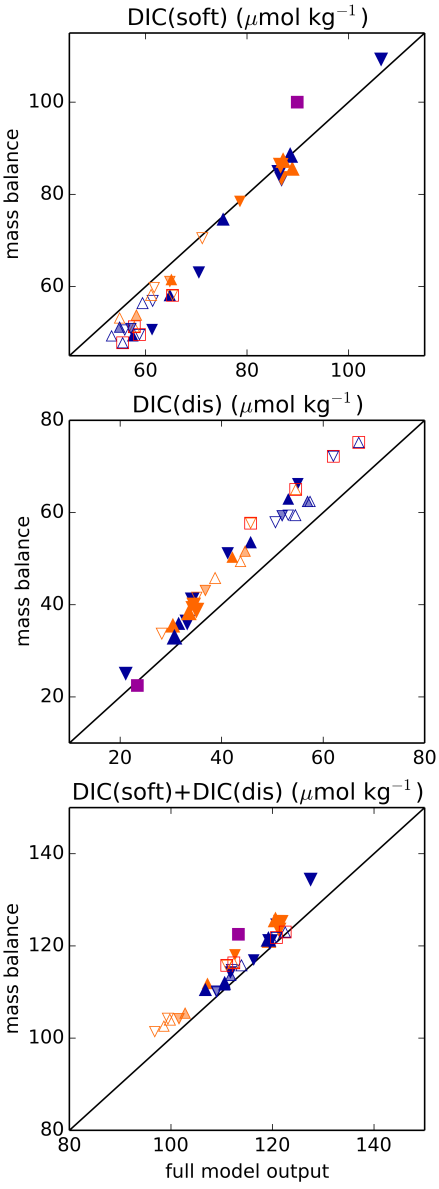

Figure 10. Using globally averaged NO_3 and the NO_3 denitrification sink as well as values of NO_{3pre} and DIC_{dis} in regions of deepwater formation in the Southern Ocean and the North Atlantic weighted by the fractions of the world oceans derived from each of these sites, it is possible to reconstruct the sum of the globally averaged DIC_{dis} and DIC_{soft}:

$$DIC_{dis_{global}} + DIC_{soft_{global}} \approx r_{C:N} \cdot (NO_{3_{global}} + NO_{3_{den,global}}) + \sum_{i=1}^{n} f_i \cdot (DIC_{dis_i} - r_{C:N} \cdot NO_{3_{pre_i}})$$

Here, we take into account upper-ocean water masses (above 1 km) in the North Pacific, North Atlantic, and Southern Ocean, as well as deep water masses in the North Atlantic and Southern Ocean. In each plot, the full model output is shown on the x-axis and the result of the mass balance approximation on the y-axis. Markers as in fig. 1 with the size of the symbols corresponding to the CO_2 level. The purple squares represents pre-industrial simulations (runs 41 – 42), and a red square around the symbol indicates runs with iron fertilization.

Biogeosciences Discuss., https://doi.org/10.5194/bg-2017-328
Manuscript under review for journal Biogeosciences
Discussion started: 19 September 2017

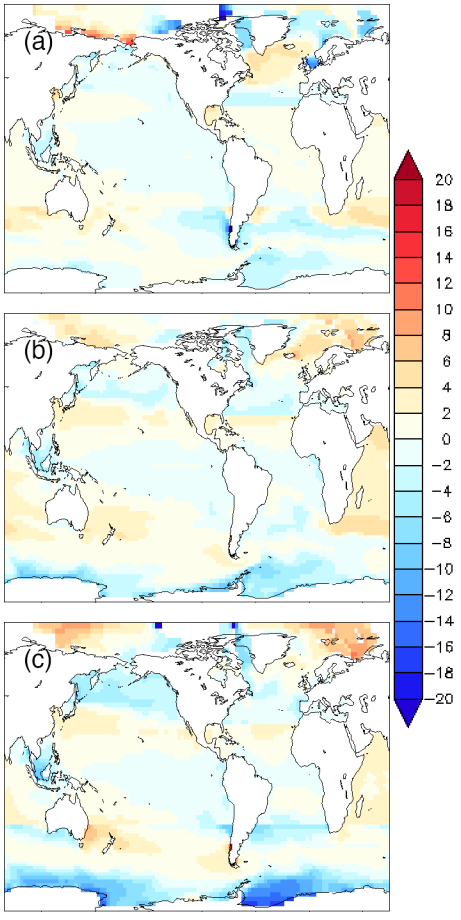

Figure 11. Shown is the difference between the exact DIC_{dis} surface field, where DIC_{sat} has been calculated using the surface alkalinity ($alk[z=0] = alk_{pre}[z=0]$) and $DIC_{soft}[z=0] = DIC_{carb}[z=0] = 0$. Differences are shown for (a) glacial; (b) interglacial; (c) $CO_2 = 911$.

Biogeosciences Discuss., https://doi.org/10.5194/bg-2017-328
Manuscript under review for journal Biogeosciences
Discussion started: 19 September 2017

Table 1. A total of 44 simulations were analyzed with varying CO_2, obliquity, precession, ice sheets (PI = pre-industrial; LGM = Last Glacial Maximum reconstruction; LGM* = topography of LGM ice sheets but with PI albedo), and with and without iron fertilization. Runs 43 and 44 and identical to 41 and 42 but the remineralization rate of sinking organic matter is reduced by 25%.

run	CO_2 (ppm)	obliquity	precession	IS	Fe	remin
1-24	180, 220, 270, 405, 607, 911	22°, 24.5°	90°, 270°	PI		
25-28	220	22°, 24.5°	90°, 270°	LGM		
29-32	180	22°, 24.5°	90°, 270°	LGM*		
33-36	180	22°, 24.5°	90°, 270°	LGM		
37-40	180	22°, 24.5°	90°, 270°	LGM	X	
41	270	23.4°	102.9°	PI		
42	270	23.4°	102.9°	PI	X	
43	270	23.4°	102.9°	PI		75%
44	270	23.4°	102.9°	PI	X	75%